

# Energy-filtered excited states and real-time dynamics served in a contour integral

Ke Liao<sup>\*,†,‡,¶</sup>

<sup>†</sup>*Faculty of Physics, Arnold Sommerfeld Centre for Theoretical Physics (ASC),*

*Ludwig-Maximilians-Universität München, Theresienstr. 37, 80333 München, Germany*

<sup>‡</sup>*Munich Center for Quantum Science and Technology (MCQST), Schellingstrasse 4, 80799*

*München, Germany*

<sup>¶</sup>*Max Planck Institute for Solid State Research, Heisenbergstraße 1, 70569 Stuttgart*

E-mail: ke.liao.whu@gmail.com

## Abstract

It is observed that the Cauchy integral formula (CIF) can be used to represent holomorphic functions of diagonalizable operators on a finite domain. This forms the theoretical foundation for applying various operators in the form of a contour integral to a state, while filtering away eigen-components that are not included by the contour. As a special case, the identity operator in the integral form—the Riesz projector—is used to design an algorithm for finding a given number of eigen-pairs whose energies are close to a specified value in the equation-of-motion coupled cluster singles and doubles (EOM-CCSD) framework, with applications to calculate core excited states of molecules which is relevant for the X-ray absorption spectroscopy (XAS). As a generalization, I showcase a novel real-time electron dynamics (RT-EOM-CCSD) algorithm based on the CIF form of the exponential time-evolution operator, which admits extremely large time steps while preserving accurate spectral information.

# Introduction

While significant progress has been made in studying excited states of molecules using quantum chemical methods over the past several decades, certain challenges persist, particularly in developing methods to efficiently find eigenstates near a specified energy value and in performing real-time dynamics that can selectively target specific portions of the eigen-spectrum. Early response theories based on real-time dynamics in Hartree-Fock (HF) and density functional theory (DFT)<sup>1-4</sup> established fundamental approaches to calculating excited states of molecules. Subsequently, similar response theories have been developed in the coupled cluster (CC) framework.<sup>5-22</sup> In the meantime, specialized techniques have also emerged to target specific excited states more directly. These include the core-valence separation approaches<sup>23-25</sup> for core excitations, energy-specific scheme,<sup>26</sup> and various shift-and-invert techniques.<sup>27-30</sup> Complementary to these methods, frequency-domain approaches based on the correction vector method,<sup>31-34</sup> damped response<sup>35,36</sup> and complex polarization propagator approaches<sup>37-42</sup> also allow direct calculation of spectral features at selected frequencies.

Based on the contour integral representation of the identity operator—the Riesz projector,<sup>43</sup> the FEAST algorithm first introduced in the context of density functional theory (DFT)<sup>44</sup> provides a systematic approach to find eigen-states within a specified energy window. However, a prior estimate of the number of eigen-states in the window is necessary for its efficiency and stability,<sup>45</sup> which can be challenging when the energy window is densely populated. Despite its success in DFT and as a general eigen-value solver, its adoption in quantum chemistry has been relatively limited, with notable applications primarily in density matrix renormalization group (DMRG)<sup>46</sup> for calculating vibrational states.

In this work, I propose an algorithm for finding  $n$  eigen-states with energies near a specified value in the framework of equation-of-motion coupled cluster singles and doubles (EOM-CCSD) theory with an adaption of the FEAST algorithm. This is achieved by dynamically adjusting the contour radius to include the desired number of eigen-states among a fixed number of trial vectors. This strategy differs from the original FEAST algorithm<sup>44</sup> or

its DMRG extension,<sup>46</sup> which aims to find all eigen-states within a fixed energy interval. To demonstrate the algorithm’s potential, I apply it to study core-excited states relevant to X-ray absorption spectroscopy (XAS), which are crucial for understanding molecular electronic structure.

More importantly, I demonstrate that the Riesz projector used in FEAST is a special case of the Cauchy integral formula (CIF), which can represent general holomorphic functions of diagonalizable operators. This observation enables much broader potential theoretical and algorithmic developments. I notice that quantum algorithms based on the CIF have been proposed in Ref.,<sup>47</sup> however, only with a focus on the quantum resource estimation and error analysis. In this work, I provide a concrete application by using the CIF to represent the time-evolution operator, resulting in a novel real-time electron dynamics algorithm in the EOM-CCSD framework that allows for significantly larger time steps while preserving accurate spectral information. This algorithm effectively filters out unwanted eigen-components from higher and lower energy states irrelevant to the dynamics of interest, making it valuable for evolving states with dominant components in densely clustered energy windows (like valence or core excited regions). The CIF approach opens numerous potential applications across quantum chemistry, condensed matter physics, and quantum information science, e.g. thermal expectation value calculations within specified energy windows,<sup>48–50</sup> calculating long-time averages of observables within narrow energy windows—central to verifying the eigenvalue thermalization hypothesis (ETH),<sup>51–54</sup> and state preparation for quantum simulations.<sup>55</sup>

The paper is organized as follows. In the Theory section, I introduce the theoretical background of the CIF and provide a brief recapitulation of the EOM-CCSD method. I then present its FEAST extension, which enables the calculation of excited states around any energy value. Additionally, I explain how the CIF-based real-time EOM-CCSD can be implemented. The details of the computational setup and the technical tools used in this work are outlined in Computational Details. In the Results and Discussion section, I

demonstrate the capability of the FEAST-EOM-CCSD algorithm by calculating the core excited states of several molecules and present a preliminary study of the CIF-based real-time electron dynamics of the H<sub>2</sub>O molecule. Finally, I conclude with a summary and discuss potential future directions for CIF-based algorithms.

## Theory

The Cauchy integral formula (CIF) is a powerful tool in complex analysis, and it states that for any holomorphic function  $f(z)$  on the complex plane, the value of  $f(a)$  at a point  $a$  inside a simple closed curve  $C$  can be calculated by the following formula

$$f(a) = \frac{1}{2\pi i} \oint_C \frac{f(z)}{z - a} dz. \quad (1)$$

A function  $f(z)$  is called holomorphic when it is differentiable at every point in its domain. When  $f(z) = 1$ , the operator version of Eq. (1) defines the Riesz projector<sup>43</sup>

$$\hat{P} \equiv \sum_{p \in \mathcal{C}} |\Psi_p\rangle \langle \Psi_p| = \frac{1}{2\pi i} \oint_C \frac{1}{z\hat{I} - \hat{A}} dz, \quad (2)$$

where  $\hat{I}$  is the identity operator and  $\hat{A}$  is in general a hermitian matrix or a hermitian operator, e.g. the Hamiltonian, with  $|\Psi_p\rangle$  being its eigen-vectors. I use the letter  $\mathcal{C}$  to indicate the set of indices of eigen-values circled by the contour  $C$ . This crucial identity enables the so-called FEAST algorithm to calculate the eigen-values and eigen-states within a specified energy window in the context of density functional theory<sup>44</sup> and in matrix product states related algorithms.<sup>46</sup> I observe that the above identity Eq. (2) is a special case and that CIF can be used to represent general holomorphic functions of diagonalizable operators on a finite domain as

$$f(\hat{A}) = \frac{1}{2\pi i} \oint_C \frac{f(z)}{z\hat{I} - \hat{A}} dz, \quad (3)$$

where  $\hat{A}$  is a diagonalizable operator and can be written in its spectral decomposition as  $\hat{A} = \sum_i a_i |\Psi_i^R\rangle \langle \Psi_i^L|$  using its right- and left-eigen-vectors. It can easily be shown that for all  $z$  on the contour  $C$  such that  $|z| > \|\hat{A}\|$ , where  $\|\hat{A}\|$  can be any matrix norm, the Taylor expansion of the resolvent  $1/(z\hat{I} - \hat{A})$  is well-defined. This corresponds to the condition that the contour  $C$  encloses all the eigen-values of  $\hat{A}$ . Therefore, using the eigen-decomposition of  $\hat{A}$  and the normal CIF, one can arrive at the above formula Eq. (3). Alternatively, if one is only interested in a part of the eigen-spectra of  $\hat{A}$ , one can define a contour  $C$  on the complex plane that encloses only the eigen-values of interest. This is equivalent to defining a new matrix  $\tilde{A} = \sum_{p \in \mathcal{C}} a_p |\Psi_p^R\rangle \langle \Psi_p^L|$  containing parts of the original eigen-components selected by the contour  $C$  and indicated by  $p \in \mathcal{C}$ .

Based on these theoretical insights, I will show that (i) the original FEAST algorithm based on the projector Eq. (2) can be adapted to the EOM-CCSD theory involving a non-Hermitian Hamiltonian with small modifications; and (ii) a novel real-time electron dynamics algorithm in the EOM-CCSD framework can be developed based on the integral form of the time-evolution operator  $e^{-i\bar{H}t} = \frac{1}{2\pi i} \oint_C \frac{e^{-z}}{z\hat{I} - i\bar{H}t} dz$ .

## EOM-CCSD

In this work, I focus on the neutral electronic excitations of a system, and I recapitulate accordingly the electronic excitation version of EOM-CCSD (EE-EOM-CCSD) theory in this subsection. I note that the theories discussed in the following subsections can be easily adapted to other versions of EOM-CCSD and potentially other methods as well, such as DFT, other quantum chemical methods and even some tensor network theories. In the rest of the paper, I will refer to the EE-EOM-CCSD theory as EOM-CCSD for simplicity.

The EOM-CCSD theory solves the following effective eigen-value problem

$$\bar{H} |\Psi_k\rangle = E_k |\Psi_k\rangle, \quad (4)$$

where  $E_k$  is the  $k$ th excitation energy corresponding to the  $k$ th excited state  $\Psi_k$ . The non-Hermitian effective Hamiltonian  $\bar{H}$  is defined as

$$\bar{H} = e^{-\hat{T}} \hat{H} e^{\hat{T}} - E_{\text{CCSD}}, \quad (5)$$

where  $E_{\text{CCSD}}$  is the CCSD ground state energy and  $\hat{T} = \sum_{ai} T_i^a \hat{a}_a^\dagger \hat{a}_i + 1/4 \sum_{abij} T_{ij}^{ab} \hat{a}_a^\dagger \hat{a}_b^\dagger \hat{a}_j \hat{a}_i$  is the cluster operator containing the singles and doubles operators, whose amplitudes are determined by solving the CCSD amplitudes equations, and  $\hat{H}$  is the second quantized Hamiltonian in a given set of orbital basis  $\{\phi_s\}$ , defined as

$$\hat{H} = \sum_{pq} h_{pq} \hat{a}_p^\dagger \hat{a}_q + \frac{1}{4} \sum_{pqrs} V_{pqrs} \hat{a}_p^\dagger \hat{a}_q^\dagger \hat{a}_s \hat{a}_r. \quad (6)$$

In the above, I follow the convention that the indices  $p, q, r, s$  run over all the orbitals,  $a, b, c, d$  run over the virtual orbitals, and  $i, j, k, l$  run over the occupied orbitals. The EOM-CCSD eigen-vectors  $|\Psi_k\rangle$  can be written as

$$|\Psi_k\rangle = |D_0\rangle + \sum_{ai} u_i^a \hat{a}_a^\dagger \hat{a}_i |D_0\rangle + \frac{1}{4} \sum_{abij} u_{ij}^{ab} \hat{a}_a^\dagger \hat{a}_b^\dagger \hat{a}_j \hat{a}_i |D_0\rangle, \quad (7)$$

where  $|D_0\rangle$  is the reference determinant, normally the Hartree-Fock determinant. The  $u_i^a$  and  $u_{ij}^{ab}$  are the amplitudes to be determined by projecting the EOM-CCSD amplitudes equation Eq. (4) to the singles and doubles subspace. Normally, the modified Davidson algorithm is used to solve the non-Hermitian eigen-value problem Eq. (4) for a few low-lying eigen-states. I refer to Refs.<sup>8-11,16,56,57</sup> for more details on the EOM-CCSD theory. In the following subsection, I will take advantage of one of the key steps in the EOM-CCSD algorithm, namely the matrix-vector multiplication  $\bar{H} |\Psi_k\rangle$ , to achieve FEAST-EOM-CCSD.

## FEAST-EOM-CCSD

The key idea of the FEAST algorithm is to use the projector Eq. (2) to project trial vectors into a subspace spanned by eigen-states whose energies are circled in by the contour  $C$ . Similarly, for the non-Hermitian  $\bar{H}$  in EOM-CCSD, the biorthogonal left- and right-eigenstates can be used to decompose the resolvent of  $\bar{H}$ . Therefore, one can define the following projector

$$\bar{P} = \sum_{p \in \mathcal{C}} |\Psi_p^R\rangle \langle \Psi_p^L| = \frac{1}{2\pi i} \oint_C \frac{1}{z\hat{I} - \bar{H}} dz, \quad (8)$$

where  $\langle \Psi_p^L|$  and  $|\Psi_p^R\rangle$  are left- and right-eigen-state associated with the eigen-value  $E_p$ , and they fullfil  $\langle \Psi_p^L | \Psi_q^R \rangle = \delta_{pq}$ . I point out that the biorthogonal formulation is used only for showing that the projector  $\bar{P}$  can indeed filter eigen-components as in a Hermitian case. Since currently only the excitation energies are of interest, I use only the right trial vectors to generate the subspace for the non-Hermitian eigen-value problem, and as in normal one-sided EOM-CCSD theory, no left eigen-vectors are calculated.

Starting from a random trial vector  $|\Phi^T\rangle$ , I can apply the projector  $\bar{P}$  on it to obtain the new state

$$|\tilde{\Phi}\rangle = \sum_{p \in \mathcal{C}} |\Psi_p^R\rangle \langle \Psi_p^L | \Phi^T \rangle = \frac{1}{2\pi i} \oint_C \frac{1}{z\hat{I} - \bar{H}} |\Phi^T\rangle dz, \quad (9)$$

which has support on  $\{|\Psi_p^R\rangle | p \in \mathcal{C}\}$  only. The two key steps are to apply  $\frac{1}{z\hat{I} - \bar{H}}$  on  $|\Phi^T\rangle$  and to carry out the contour integral in an efficient and accurate way. They can be achieved by recasting the integral into a weighted summation along a set of  $K$  Gauss-Legendre quadrature nodes on the circle  $C$ , see the upper panel of Fig. 1,

$$|\tilde{\Phi}\rangle \approx \frac{1}{2} \sum_{e=1}^{K/2} \omega_e \text{Re} (E_r e^{i\theta_e} |Q_e\rangle), \quad (10)$$

where  $z_e$ ,  $\theta_e$  and  $\omega_e$  are the coordinate, the angle and the weight at quadrature node  $e$ ,  $E_r$

is the current radius of the contour, and  $|Q_e\rangle$  is the solution of the following linear system

$$(z_e \hat{I} - \bar{H}) |Q_e\rangle = |\Phi^T\rangle. \quad (11)$$

One can generate  $n$  different trial vectors following the above recipe and orthogonalize them <sup>1</sup>, with which the matrix elements of  $\bar{\mathbf{H}}^{\text{eff}}$  in the subspace can be calculated as

$$\bar{H}_{ij}^{\text{eff}} = \langle \tilde{\Phi}_i | \bar{H} | \tilde{\Phi}_j \rangle - E_{\text{CCSD}} \delta_{ij}. \quad (12)$$

Solving the following non-Hermitian eigen-value problem

$$\bar{\mathbf{H}}^{\text{eff}} |\Psi_p\rangle = E_p |\Psi_p\rangle \quad (13)$$

yields eigen-values  $E_p$  within the desired energy window defined by the contour  $C$ .

In contrast to the original FEAST algorithm,<sup>44,45</sup> which relies on a prior estimate of the number of eigen-states within a specified energy window for convergence and stability, I adopt a different strategy of finding a given number of eigen-states whose energies are close to a specified value. This is achieved by dynamically adjusting the contour radius using the current estimate of eigen-values and the specified energy value. I outline the FEAST-EOM-CCSD algorithm in Table 1. In practice, I find that the more accurately the linear systems are solved, the faster the algorithm converges. Typically, I use 5-20 iterations per linear system, depending on how well-conditioned the linear systems are. The  $m$  supplemental trial vectors are used to ensure that possible degeneracies around the largest and smallest eigen-values are resolved for the  $n$  eigen-states. They also improve the overall convergence of the algorithm. I demonstrate the algorithm's effectiveness using the H<sub>2</sub>O molecule with a minimal basis set in Fig. 2 (Left), targeting low-lying eigenvalues around a specific value of  $E_c = 38.096$  eV and comparing the results with reference EOM-CCSD eigenvalues. This benchmarks FEAST-

---

<sup>1</sup>In contrast to the original FEAST algorithm, which does not require orthogonalization of the trial vectors, I find that using orthogonalized trial vectors improves stability of the overall algorithm.



Table 1: Steps of the FEAST-EOM-CCSD algorithm.

Step	Description
1	Choose an energy center $E_c$ and the number $n$ of eigen-states to target around it.
2	Generate $n$ random trial vectors and optionally also a small number $m$ of supplemental random trial vectors, $\{ \Phi_i^T\rangle\}, i = 1, \dots, n+m$ , and choose the initial contour radius $E_r$ to be a large value, e.g. 1 Ha.
3	Generate 5 (effectively $K=10$ as conjugation relation is used) Gauss-Legendre nodes $\{x_e\}$ between $[-1,1]$ and their associated weights $\{w_e\}$ ; Calculate the complex nodes' coordinates by $z_e = E_c + E_r \exp(i\theta_e)$ , where $\theta_e = -\frac{\pi}{2}(x_e - 1)$ .
4	For each trial vector $ \Phi_i^T\rangle, i = 1, \dots, n+m$ , solve the linear system problem $(z_e \hat{I} - \bar{H}) Q_e\rangle =  \Phi_i^T\rangle$ at each quadrature node $e$ and obtain the new trial vector $ \tilde{\Phi}_i\rangle \leftarrow \frac{1}{2} \sum_{e=1}^{K/2} \omega_e \text{Re}(E_r e^{i\theta_e}  Q_e\rangle)$ .
5	Use the QR decomposition <sup>58</sup> to orthogonalize the trial vectors $\{\tilde{\Phi}_i\}$ and calculate the $\bar{\mathbf{H}}^{\text{eff}}$ elements in the subspace spanned by $\{ \tilde{\Phi}_i\rangle\}$ .
6	Diagonalize the $\bar{\mathbf{H}}$ of size $(n+m) \times (n+m)$ to obtain the eigen-values $\{\lambda_i\}$ and eigen-vectors $\{\mathbf{c}_i\}, i = 1, 2, \dots, n+m$ .
7	Update the trial vectors using the eigen-vectors: $ \Phi_i^T\rangle \leftarrow \sum_{j=1}^n c_i^j  \tilde{\Phi}_j\rangle$ .
8	Update $E_r$ such that $n$ current eigen-values closest to $E_c$ are circled, by calculating and sorting the distances $d =  \lambda_i - E_c $ and choosing the $n$ th as the new $E_r \leftarrow d_n$ .
9	Check if convergence is reached, i.e. the change in the norm of the $n$ eigen-values between two consecutive cycles is smaller than a threshold $\epsilon$ . If not, go to step 3.

EOM-CCSD's ability to accurately target eigenvalues without calculating the lower-energy states. Additionally, I show the convergence of a core-excitation energy near  $E_c = 535.50$  eV for the H<sub>2</sub>O molecule using the aug-cc-pVTZ basis set in Fig. 2 (Right). The core-excitation is identified by its dominant component in the eigen-vector, corresponding to the transition  $1a_1 \rightarrow 4a_1$  between the orbitals.

## CIF-based real-time EOM-CCSD (RT-EOM-CCSD)

Although the effective Hamiltonian  $\bar{H}$  is non-Hermitian, its eigen-values are real<sup>2</sup>, since the similarity transformation preserves the real eigen-values of the original Hamiltonian. Hence applying the time-evolution operator  $\exp(-i\bar{H}t)$  onto a state does not alter its norm. Real-time electron dynamics within the EOM-CCSD framework has been studied by several

<sup>2</sup>In a truncated space, such as the singles and doubles space used in EOM-CCSD, the diagonalization can sometimes lead to complex eigen-values.

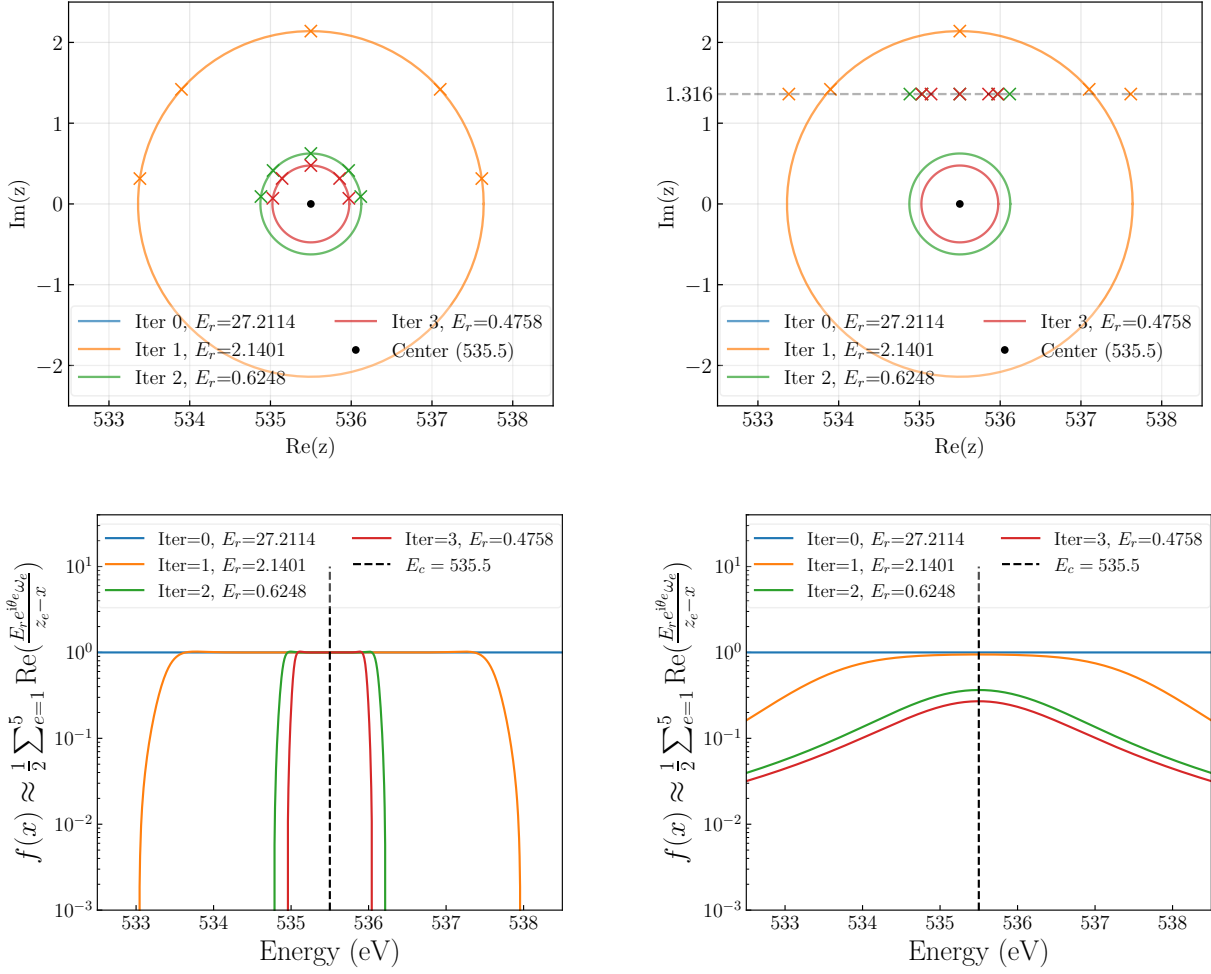


Figure 1: Energy filtering effect of applying the projector  $\bar{P}$ , demonstrated using 10 Gauss-Legendre quadrature nodes on the contour  $C$  (only 5 nodes are shown and the conjugation relation is applied) with varying radii  $E_r$  while keeping a constant number of eigen-states  $n = 5$  around the energy center  $E_c = 535.5$  eV as the iterations proceed. (Left) The filtering function  $f(x) \approx \frac{1}{2} \sum_{e=1}^5 \text{Re}(\frac{E_r e^{i\theta_e \omega_e}}{z_e - x})$ . (Right) The same filtering function, but limiting the magnitude of the imaginary part of  $z_e$  to be not smaller than 0.05 Ha (1.361 eV).

groups,<sup>12,17,18,59</sup> based on the time-dependent Schrödinger equation.

In this work, I realize the real-time electron dynamics by applying the following integral form of the time-evolution operator

$$\hat{U}(t) = \exp(-i\bar{H}t) = \frac{1}{2\pi i} \oint_C \frac{e^{-z}}{z\hat{I} - i\bar{H}t} dz. \quad (14)$$

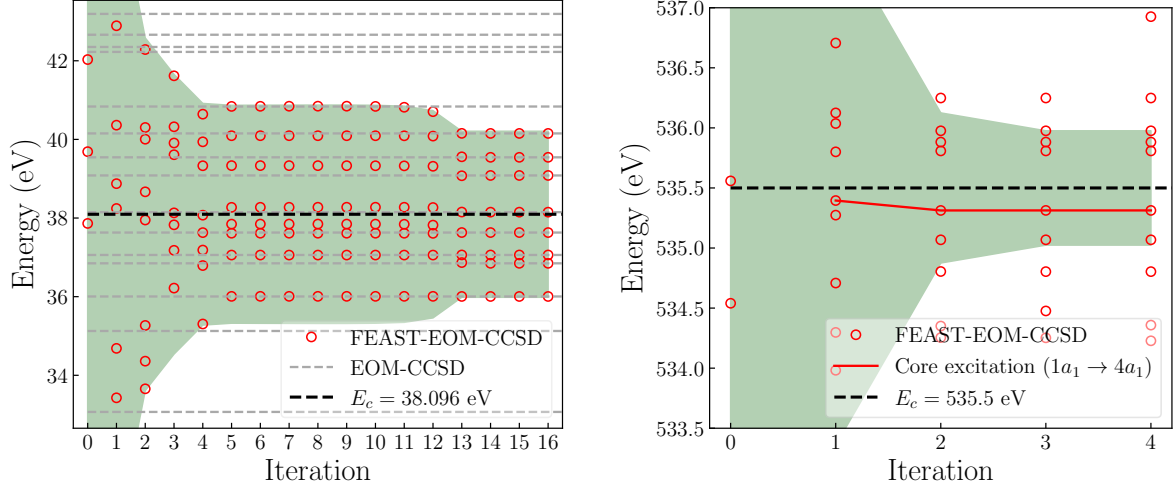


Figure 2: FEAST-EOM-CCSD targetting low-lying and core excitation energies of the  $\text{H}_2\text{O}$  molecule. ( Left) Benchmarking FEAST-EOM-CCSD against EOM-CCSD by calculating 8 low-lying excitation energies near  $E_c = 1.4$  Ha using the STO-6G basis set. (Right) FEAST-EOM-CCSD targetting 5 highly-excited states around  $E_c = 535.5$  eV using the aug-cc-pVTZ basis set. The core excitation ( $1a_1 \rightarrow 4a_1$ ) energy is marked by the red line. The grey dashed lines are the reference EOM-CCSD eigen-values on the left figure and the red dots are the FEAST-EOM-CCSD eigen-values in both figures. The green shaded area is the dynamically adjusted energy window in both figures.

When the contour  $C$  encloses the whole spectrum of  $i\bar{H}t$ , this formulation is exact. In practice, as in many scenarios, one is only interested in a certain part of the whole spectra. Therefore, one can choose the contour  $C$  to define the energy window of interest<sup>3</sup>. Using a similar argument as in FEAST-EOM-CCSD, one can show that the above operator filters the eigen-components whose energies are outside the contour  $C$  and evolves the initial state with the eigen-components whose energies are within the contour  $C$  only:

$$\begin{aligned}
 |\Phi(t)\rangle &= \tilde{U}(t) |\Phi(0)\rangle \\
 &= \sum_{p \in C} e^{-iE_p t} |\Psi_p^R\rangle \langle \Psi_p^L | \Phi(0)\rangle,
 \end{aligned} \tag{15}$$

where I use  $\tilde{U}$  to indicate that the time-evolution operator now only evolves a part of all the

<sup>3</sup>Notice that the eigen-values of  $i\bar{H}t$  lie on the imaginary axis. Hence, the contour should be centered accordingly.

eigen-components. Following the steps outlined in FEAST-EOM-CCSD, to apply  $\frac{e^{-z}}{z\hat{I}-i\hat{H}\Delta t}$  on the initial state  $|\Phi(t=0)\rangle$  and to carry out the contour integral in an efficient and accurate way, one can again recast the integral into a weighted summation along a set of  $K$  Gauss-Legendre quadrature nodes on the circle  $C$

$$|\Phi(\Delta t)\rangle \approx \frac{1}{2} \sum_{e=1}^K \omega_e E_r \Delta t e^{i\theta_e} |Q_e\rangle, \quad (16)$$

with the  $z_e$  being dependent on  $\Delta t$  to account for the time evolution and  $|Q_e\rangle$  being the solution of the following linear system problem

$$(z_e \hat{I} - i\hat{H}\Delta t) |Q_e\rangle = e^{-z_e} |\Phi(0)\rangle. \quad (17)$$

As long as the linear systems are solved accurately and the quadrature errors are small, in theory, the time evolved state by  $\tilde{U}$  suffers from little to no time step errors. The Gauss-Legendre quadrature nodes ensure that with  $K$  nodes within a finite length, a polynomial of degree  $2K-1$  can be integrated exactly along this line. When one chooses the contour  $C$  to be away from the poles of the resolvent, the integrand  $e^{-z}/(z\hat{I}-i\hat{H}\Delta t)$  is a smooth function on the contour, and the quadrature error is well controlled by choosing an appropriate number of  $K$  nodes. See Ref.<sup>47</sup> for detailed analysis on the quadrature error. This enables very large time steps to be used for evolving the system, up to the timescale determined by the fastest dynamics of interest.

Currently, I adopt the scheme to update the state repeatedly by the time-evolution operator with a fixed time step  $\Delta t$ . In principle, however, one can also apply the time-evolution operator at different time values to the initial state to obtain the evolved state at any time. One potential drawback of this scheme is that the contour will be very large at long times, and the linear systems at nodes with large real parts will be very difficult to solve accurately. I leave the investigation along this line to future work.

## Computational details

In the FEAST-EOM-CCSD algorithm, I use  $K = 10$  Gauss-Legendre quadrature nodes. In practice, exploiting the conjugation symmetry of nodes across the real axis reduces the number of linear systems from 10 to 5. However, in the CIF-based RT-EOM-CCSD algorithm, in order to reduce the quadrature error,  $K = 16$  Gauss-Legendre nodes are used. In the meantime, the poles of  $\frac{e^{-z}}{z - iH\Delta t}$  are on the imaginary axis, no such conjugation relation can be used. Therefore, one needs to solve  $K$  linear systems for each time step. All geometries are optimized at the CCSD level of theory using the TZVP basis set and can be accessed at.<sup>60</sup> I use the generalized conjugate residual with inner orthogonalization and outer truncation (GCROT)<sup>61</sup> and a version of the generalized minimal residual method (LGMRES)<sup>62</sup> to solve the linear systems, as implemented in the SciPy library.<sup>63</sup> The latter performs better when the linear system is ill-conditioned.

In the FEAST-EOM-CCSD algorithm, the linear systems become ill-conditioned when contour nodes lie close to Hamiltonian eigen-values on the real axis. With large radii, only two nodes typically approach eigen-values, posing minimal challenges for convergence. However, complications arise with small radii, particularly when targeting core-excitation energies surrounded by numerous valence excitations in large basis sets and a small fixed number of eigen-states are sought by dynamically reducing the radius of the contour, see Fig 1. The condition number

$$\kappa(z_e \hat{I} - \bar{H}) = \frac{\max_{\lambda \in \text{spec}(\bar{H})} |z_e - \lambda|}{\min_{\lambda \in \text{spec}(\bar{H})} |z_e - \lambda|} \quad (18)$$

quantifies this difficulty, indicating solution sensitivity to perturbations. When  $z_e$  approaches near-degenerate eigen-values, the denominator approaches zero, creating ill-conditioned systems. To address this, I implement a constraint limiting the imaginary component of  $z_e$  to a minimum threshold  $\delta$  (typically 0.05-0.1 Ha), ensuring a finite denominator in  $\kappa$  and well-conditioned linear systems. This technique enables convergence even with near degeneracies present, albeit more slowly than in a well-conditioned case, e.g. using a small basis set when

there are not so many valence excitations around a core excitation.

Fig. 1 illustrates how this constraint affects the energy filtering function, defined as a discrete approximation to Eq. (1) using 10 Gauss-Legendre quadrature nodes and assuming  $f(x) = 1$ , corresponding to the operator  $\bar{P}$  used in FEAST-EOM-CCSD algorithm. It reads

$$f(x) \approx \frac{1}{2} \sum_{e=1}^5 \text{Re} \left( \frac{E_r e^{i\theta_e \omega_e}}{z_e - x} \right). \quad (19)$$

In Fig. 1, the upper panels show where the nodes are located without and with the constraint, respectively; the lower panels show the energy filtering function Eq. (19) without and with the constraint. Without the constraint, the function is sharp, filtering eigen-values outside the energy window defined by  $E_c$  and  $E_r$ . With the constraint, the function becomes less sharp but still suppresses eigen-values outside the window, allowing convergence to the correct eigen-values. This technique is used to obtain core-excitation energies of molecules in the aug-cc-pVTZ basis set, as shown in Table 3.

The algorithms are implemented in PyMES.<sup>64–66</sup> I use a modified PySCF<sup>67,68</sup> code to perform mean-field HF calculations, to generate the integrals<sup>69</sup> and to realize the matrix-vector multiplication in EOM-CCSD.

## Results and Discussion

### Core excitation energies

Table 2: Core excitation ( $1a_1 \rightarrow 4a_1$ ) energies (eV) of the H<sub>2</sub>O molecule in various basis sets

Basis	FEAST	ES <sup>a</sup>	EOM-CCSD	Exp. <sup>b</sup>
6-311G**	535.74	535.72	535.76 <sup>c</sup>	534.00
cc-pVTZ	535.42	535.41	535.34 <sup>d</sup>	
aug-cc-pVTZ	535.31	535.30	535.32 <sup>e</sup>	

<sup>a</sup> Data from Ref.<sup>26</sup> <sup>b</sup> Data from Ref.<sup>70</sup> <sup>c</sup> Data from Ref.<sup>71</sup> <sup>d</sup> Data from Ref.<sup>72</sup> <sup>e</sup> Data from Ref.<sup>73</sup>

In Table 2, the oxygen K-edge absorption energies of the water molecule in various basis

Table 3: Core excitation energies (eV) of the N<sub>2</sub>, CO, C<sub>2</sub>H<sub>2</sub>.

Molecule	FEAST		ES <sup>a</sup>	CVS <sup>b</sup>	EOM <sup>c</sup>	Exp.
	6-311G**	aug-cc-pVTZ				
N <sub>2</sub> ( $1\sigma_u \rightarrow 1\pi_g$ )	402.17	401.67	401.93	402.04	402.04	400.96 <sup>d</sup>
CO ( $2\sigma \rightarrow 2\pi$ )	288.34	287.61	287.99	288.18	288.21	287.40 <sup>e</sup>
C <sub>2</sub> H <sub>2</sub> ( $1\sigma_u \rightarrow 1\pi(2p)$ )	286.96	286.47	286.70	-	-	285.81 <sup>f</sup>

<sup>a</sup> Data from Ref.,<sup>26</sup> with modified Sadlej basis set. <sup>b</sup> Data from Ref.,<sup>24</sup> with aug-cc-pCVTZ+Rydberg basis set. <sup>c</sup> Data from Ref.<sup>24,41</sup> using aug-cc-pCVTZ+Rydberg for N<sub>2</sub> and aug-cc-pCVTZ for CO. <sup>d</sup> Data from Ref.<sup>74</sup> <sup>e</sup> Data from Ref.<sup>75</sup> <sup>f</sup> Data from Ref.<sup>76</sup>

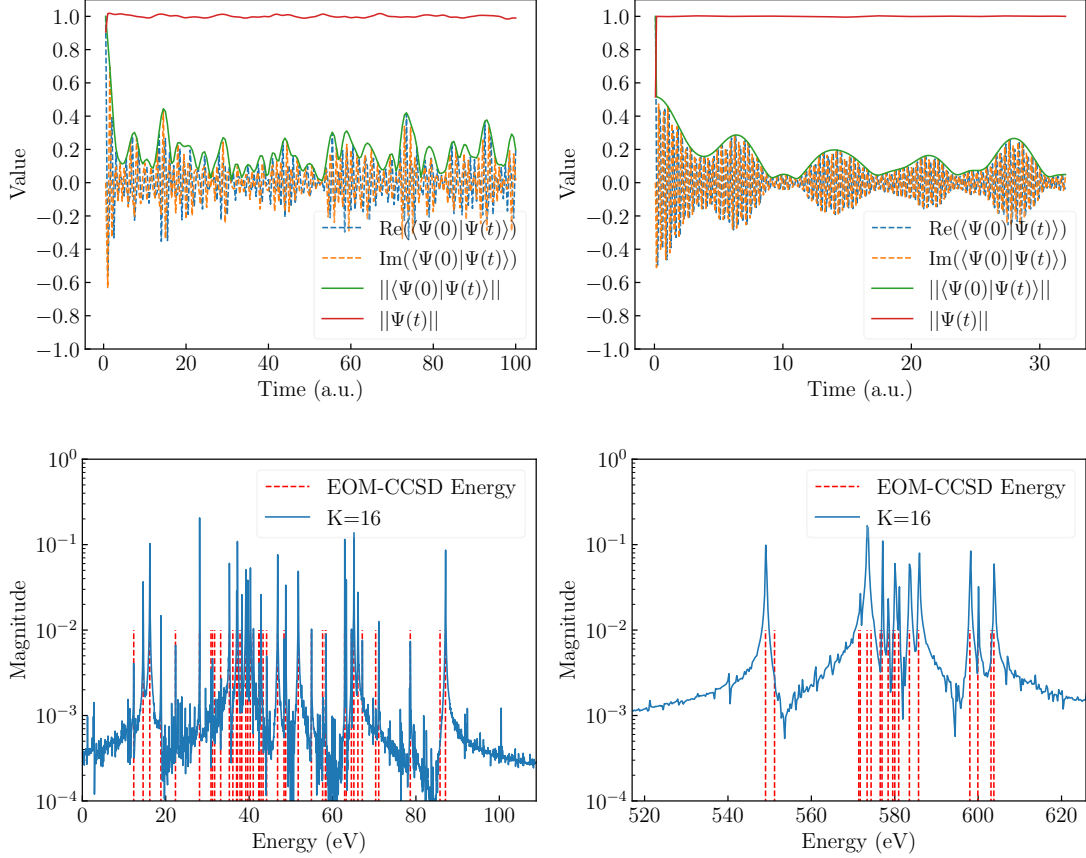


Figure 3: Upper: The electron dynamics of the H<sub>2</sub>O molecule in the STO-6G basis set with random initial states for valence (left) and core (right) energy regions. The time steps used are 0.5 a.u. and 0.08 a.u. for the valence and core excited states, respectively. In total 8000 steps are used for both cases (not plotted in full). After each step, the state is normalized to 1 to avoid the norm drift. Lower: The Fourier transform of the real-time electron dynamics for valence excited state spectra (left) and the core excited state spectra (right). The energy windows used for time-evolution are -27.211 eV–136.057 eV (-1 Ha–5 Ha) and 272.114 eV–816.342 eV (10 Ha–30 Ha) for the valence and core spectra, respectively.  $K = 16$  Gauss-Legendre quadrature nodes are used.

sets are calculated using the FEAST-EOM-CCSD algorithm, compared against those by the energy-specific EOM-CCSD (ES-EOM-CCSD),<sup>26</sup> the canonical EOM-CCSD<sup>71-73</sup> and the experimental value.<sup>70</sup> In theory, at convergence, the FEAST-EOM-CCSD and the ES-EOM-CCSD algorithm should agree with each other exactly, because they do not make additional approximations to the Hamiltonian. The small differences in the energies between the two algorithms can be attributed to the slightly different geometries used.

After benchmarking the new algorithm against existing methods in the same basis sets, I further apply the FEAST-EOM-CCSD algorithm to calculate the core excitation energies of the N<sub>2</sub>, CO, and C<sub>2</sub>H<sub>2</sub> molecules in the 6-311G\*\* and aug-cc-pVTZ basis sets. The results are shown in Table 3. Using the diffused basis set aug-cc-pVTZ, the calculated core excitation energies are getting closer to agreement with the experimental values. Choosing an appropriate basis set that accurately describes orbital relaxation effects is crucial for predicting core excitation energies. Accurately describing orbital relaxation effects through appropriate basis set selection is crucial but non-trivial.<sup>77</sup> CVS-EOM-CCSD<sup>23-25</sup> is a well-established method for calculating core excitations efficiently and accurately by decoupling the core excitations from the valence excitations. Since the CVS-EOM-CCSD and the full EOM-CCSD methods show very good agreement in these cases, I attribute the small differences in the energies between FEAST-EOM-CCSD, ES-EOM-CCSD and CVS-EOM-CCSD to the different basis sets and geometries used. Due to the high density of states around the core excitations when a large basis set is used, the convergence of the FEAST-EOM-CCSD algorithm can be slow. Without the stabilization technique described in Computational Details, the algorithm may fail to converge. This underscores the importance of removing the valence excitation space when calculating core excitation energies, as CVS-EOM-CCSD does. Similar to FEAST-EOM-CCSD, ES-EOM-CCSD can also target any specific energy regions by selecting trial vectors based on their energies. To converge the calculated energies, ES-EOM-CCSD requires an increasingly large number of trial vectors to be used, which can be memory and computationally expensive. In the future, more efficient and accurate



algorithms can potentially be developed by combining the strengths from CVS-, ES- and FEAST-EOM-CCSD.

## CIF-based real-time electron dynamics

Due to the many time steps needed for resolving accurately all the energy peaks, I present only preliminary results of the CIF-based real-time electron dynamics on the  $\text{H}_2\text{O}$  molecule in a minimal basis set. I Fourier transform the overlap between the initial and evolved states to obtain the spectra and compare the peaks with the excitation energies computed by the EOM-CCSD. On the upper panel of Fig. 3, I show the dynamics of two random initial states evolved for 8000 steps with a time step size of 0.5 a.u. and 0.08 a.u. for the valence (left) and core (right) excited states, respectively. To put these numbers in context, typically a time step size of 0.01 a.u. is used for electron dynamics involving core excitations.<sup>17,59</sup> I normalize the state after each time step to avoid the norm drift. The small fluctuations in the norm of the state testify the quality of the time-evolution operator in the integral form. Comparatively speaking, the fluctuations in the norm is slightly larger in the valence excited state case than in the core excited state case. Considering the extremely large time step size used, 0.5 a.u., this is expected. The energy windows used for the time-evolutions are -27.211 eV–136.057 eV (-1 Ha–5 Ha) and 272.114 eV–816.342 eV (10 Ha–30 Ha) for the valence and core spectra, respectively. The Fourier transform of the overlap between the initial and evolved state  $\langle \Phi(0) | \Phi(t) \rangle$ <sup>78</sup> are shown on the lower panel of Fig. 3 for the valence (left) and core (right) excited states. Most of the energy peaks within the energy windows are resolved accurately, with a few small valence excitation peaks being obscured by the noise. This could be due to the fact that these peaks correspond to eigen-components with very small weights in the initial random state. In practice, one can always choose an initial state with dominant components in the energy window of interest to avoid this issue.

## Conclusion

In this work, relying on the operator version of the CIF as the theoretical foundation for representing holomorphic functions of diagonalizable operators, I linked the original FEAST algorithm with a much broader class of algorithms which involve applying functions of diagonalizable operators to a state. Based on this theoretical insight, two novel algorithms were proposed—FEAST-EOM-CCSD and CIF-based RT-EOM-CCSD. I benchmarked the FEAST-EOM-CCSD against EOM-CCSD in calculating low-lying eigen-states in a small system, and further demonstrated its capability in finding the core excited states in several molecules, which are relevant to the X-ray spectroscopy. The results agree with other methods, e.g. ES-EOM-CCSD, CVS-EOM-CCSD and EOM-MRCCSD, as well as with experiments. FEAST-EOM-CCSD is highly parallelizable at different levels. For example, states around different energy centers can be calculated in parallel, the Riesz projector can be applied to each trial vector independently while the underlying linear systems can also be solved independently. Immediate improvement on the efficiency can be achieved by using low-scaling approximations<sup>26</sup> to find better initial trial vectors and to boost the efficiency of the linear system solver. I believe that the FEAST-EOM-CCSD algorithm will inspire further developments in the study of excited states in quantum chemistry and beyond.

In addition, I reported the first realization of the CIF-based real-time evolution algorithm and applied it to the water molecule to target two energy-separated spectral groups independently with extremely large time step sizes. The large time step sizes are possible due to the effective Gauss-Legendre quadrature nodes used for integration. I showed that densely packed spectra in the valence and core excited regions can be accurately resolved once long time data of the overlap between the initial and time-evolved states are gathered. I emphasize that the CIF-based real-time electron dynamics algorithm is a new approach to realize real-time electron dynamics, and it could be extended to tensor network theories such as DMRG. Its comparative advantages and disadvantages in this context over other methods, such as the time-dependent variational principle<sup>79–82</sup> and Runge-Kutta,<sup>83</sup> are yet

to be explored. I envision that the CIF-based real-time electron dynamics algorithm could also provide insights into curbing the entanglement growth in tensor network algorithms for simulating the long time dynamics of quantum many-body systems.<sup>84</sup> Its relationship to other theories that use the complex time for evolution remains to be understood.<sup>78,84</sup> Finally, other theories and algorithms that can be cast into the CIF form will also be explored.

*Acknowledgement.* K.L. would like to express gratitude towards Christian Schilling for his support on this work. Comments from Haibo Ma, Daniel Kats, Felix Hummel and Ali Alavi are also appreciated. Financial support from the German Research Foundation (Grant SCHI 1476/1-1) is gratefully acknowledged.

## References

- (1) McLACHLAN, A. D.; BALL, M. A. Time-Dependent Hartree—Fock Theory for Molecules. *Reviews of Modern Physics* **1964**, *36*, 844–855, Publisher: American Physical Society.
- (2) Schönhammer, K.; Gunnarsson, O. Time-dependent approach to the calculation of spectral functions. *Physical Review B* **1978**, *18*, 6606–6614.
- (3) Runge, E.; Gross, E. K. U. Density-Functional Theory for Time-Dependent Systems. *Physical Review Letters* **1984**, *52*, 997–1000, Publisher: American Physical Society.
- (4) Akama, T.; Nakai, H. Short-time Fourier transform analysis of real-time time-dependent Hartree–Fock and time-dependent density functional theory calculations with Gaussian basis functions. *The Journal of Chemical Physics* **2010**, *132*, 054104.
- (5) Monkhorst, H. J. Calculation of properties with the coupled-cluster method. *International Journal of Quantum Chemistry* **1977**, *12*, 421–432, Publisher: John Wiley & Sons, Ltd.

- (6) Dalgaard, E.; Monkhorst, H. J. Some aspects of the time-dependent coupled-cluster approach to dynamic response functions. *Physical Review A* **1983**, *28*, 1217–1222, Publisher: American Physical Society.
- (7) Koch, H.; Jørgensen, P. Coupled cluster response functions. *The Journal of Chemical Physics* **1990**, *93*, 3333–3344.
- (8) Stanton, J. F.; Bartlett, R. J. The equation of motion coupled-cluster method. A systematic biorthogonal approach to molecular excitation energies, transition probabilities, and excited state properties. *The Journal of Chemical Physics* **1993**, *98*, 7029–7039.
- (9) Bartlett, R. J.; Musiał, M. Coupled-cluster theory in quantum chemistry. *Reviews of Modern Physics* **2007**, *79*, 291–352, Publisher: American Physical Society.
- (10) Krylov, A. I. Equation-of-Motion Coupled-Cluster Methods for Open-Shell and Electronically Excited Species: The Hitchhiker’s Guide to Fock Space. *Annual Review of Physical Chemistry* **2008**, *59*, 433–462, Publisher: Annual Reviews.
- (11) Bartlett, R. J. Coupled-cluster theory and its equation-of-motion extensions. *WIREs Computational Molecular Science* **2012**, *2*, 126–138, reprint: <https://onlinelibrary.wiley.com/doi/pdf/10.1002/wcms.76>.
- (12) Sonk, J. A.; Caricato, M.; Schlegel, H. B. TD-CI Simulation of the Electronic Optical Response of Molecules in Intense Fields: Comparison of RPA, CIS, CIS(D), and EOM-CCSD. *The Journal of Physical Chemistry A* **2011**, *115*, 4678–4690, Publisher: American Chemical Society.
- (13) Kvaal, S. Ab initio quantum dynamics using coupled-cluster. *The Journal of Chemical Physics* **2012**, *136*, 194109.
- (14) Lopata, K.; Van Kuiken, B. E.; Khalil, M.; Govind, N. Linear-Response and Real-Time Time-Dependent Density Functional Theory Studies of Core-Level Near-Edge

- X-Ray Absorption. *Journal of Chemical Theory and Computation* **2012**, *8*, 3284–3292, Publisher: American Chemical Society.
- (15) Pigg, D. A.; Hagen, G.; Nam, H.; Papenbrock, T. Time-dependent coupled-cluster method for atomic nuclei. *Physical Review C* **2012**, *86*, 014308, Publisher: American Physical Society.
- (16) Helgaker, T.; Jørgensen, P.; Olsen, J. *Molecular Electronic-Structure Theory*; John Wiley & Sons, Ltd, 2014; pp 648–723.
- (17) Nascimento, D. R.; DePrince, A. E. Linear Absorption Spectra from Explicitly Time-Dependent Equation-of-Motion Coupled-Cluster Theory. *Journal of Chemical Theory and Computation* **2016**, *12*, 5834–5840.
- (18) Nascimento, D. R.; DePrince, A. E. I. Simulation of Near-Edge X-ray Absorption Fine Structure with Time-Dependent Equation-of-Motion Coupled-Cluster Theory. *The Journal of Physical Chemistry Letters* **2017**, *8*, 2951–2957, Publisher: American Chemical Society.
- (19) Pedersen, T. B.; Kvaal, S. Symplectic integration and physical interpretation of time-dependent coupled-cluster theory. *The Journal of Chemical Physics* **2019**, *150*, 144106.
- (20) Kristiansen, H. E.; Schøyen, S.; Kvaal, S.; Pedersen, T. B. Numerical stability of time-dependent coupled-cluster methods for many-electron dynamics in intense laser pulses. *The Journal of Chemical Physics* **2020**, *152*, 071102.
- (21) Skeidsvoll, A. S.; Balbi, A.; Koch, H. Time-dependent coupled-cluster theory for ultra-fast transient-absorption spectroscopy. *Physical Review A* **2020**, *102*, 023115, Publisher: American Physical Society.
- (22) Sverdrup Ofstad, B.; Aurbakken, E.; Sigmundson Schøyen, S.; Kristiansen, H. E.; Kvaal, S.; Pedersen, T. B. Time-dependent coupled-cluster

- theory. *WIREs Computational Molecular Science* **2023**, *13*, e1666, reprint: <https://onlinelibrary.wiley.com/doi/pdf/10.1002/wcms.1666>.
- (23) Cederbaum, L. S.; Domcke, W.; Schirmer, J. Many-body theory of core holes. *Physical Review A* **1980**, *22*, 206–222, Publisher: American Physical Society.
  - (24) Coriani, S.; Koch, H. Communication: X-ray absorption spectra and core-ionization potentials within a core-valence separated coupled cluster framework. *The Journal of Chemical Physics* **2015**, *143*, 181103.
  - (25) Vidal, M. L.; Feng, X.; Epifanovsky, E.; Krylov, A. I.; Coriani, S. New and Efficient Equation-of-Motion Coupled-Cluster Framework for Core-Excited and Core-Ionized States. *Journal of Chemical Theory and Computation* **2019**, *15*, 3117–3133, Publisher: American Chemical Society.
  - (26) Peng, B.; Lestrangle, P. J.; Goings, J. J.; Caricato, M.; Li, X. Energy-Specific Equation-of-Motion Coupled-Cluster Methods for High-Energy Excited States: Application to K-edge X-ray Absorption Spectroscopy. *Journal of Chemical Theory and Computation* **2015**, *11*, 4146–4153, Publisher: American Chemical Society.
  - (27) Yu, X.; Pekker, D.; Clark, B. K. Finding Matrix Product State Representations of Highly Excited Eigenstates of Many-Body Localized Hamiltonians. *Physical Review Letters* **2017**, *118*, 017201, Publisher: American Physical Society.
  - (28) Dorando, J. J.; Hachmann, J.; Chan, G. K.-L. Targeted excited state algorithms. *The Journal of Chemical Physics* **2007**, *127*, 084109.
  - (29) Booth, G. H.; Chan, G. K.-L. Communication: Excited states, dynamic correlation functions and spectral properties from full configuration interaction quantum Monte Carlo. *The Journal of Chemical Physics* **2012**, *137*, 191102.

- (30) Zhao, L.; Neuscamman, E. Variational Excitations in Real Solids: Optical Gaps and Insights into Many-Body Perturbation Theory. *Physical Review Letters* **2019**, *123*, 036402.
- (31) Kühner, T. D.; White, S. R. Dynamical correlation functions using the density matrix renormalization group. *Physical Review B* **1999**, *60*, 335–343, Publisher: American Physical Society.
- (32) McClain, J.; Lischner, J.; Watson, T.; Matthews, D. A.; Ronca, E.; Louie, S. G.; Berkelbach, T. C.; Chan, G. K.-L. Spectral functions of the uniform electron gas via coupled-cluster theory and comparison to the \$GW\$ and related approximations. *Physical Review B* **2016**, *93*, 235139, Publisher: American Physical Society.
- (33) Lewis, A. M.; Berkelbach, T. C. Ab Initio Lifetime and Concomitant Double-Excitation Character of Plasmons at Metallic Densities. *Physical Review Letters* **2019**, *122*, 226402, Publisher: American Physical Society.
- (34) Lee, S.; Zhai, H.; Chan, G. K.-L. An Ab Initio Correction Vector Restricted Active Space Approach to the L-Edge XAS and 2p3d RIXS Spectra of Transition Metal Complexes. *Journal of Chemical Theory and Computation* **2023**, *19*, 7753–7763, Publisher: American Chemical Society.
- (35) Kristensen, K.; Kauczor, J.; Kjærgaard, T.; Jørgensen, P. Quasienergy formulation of damped response theory. *The Journal of Chemical Physics* **2009**, *131*, 044112.
- (36) Schnack-Petersen, A. K.; Moitra, T.; Folkestad, S. D.; Coriani, S. New Implementation of an Equation-of-Motion Coupled-Cluster Damped-Response Framework with Illustrative Applications to Resonant Inelastic X-ray Scattering. *The Journal of Physical Chemistry A* **2023**, *127*, 1775–1793, Publisher: American Chemical Society.
- (37) Norman, P.; Bishop, D. M.; Jørgensen, H.; Oddershede, J. Near-resonant absorption in the time-dependent self-consistent field and multiconfigurational self-

- consistent field approximations. *The Journal of Chemical Physics* **2001**, *115*, 10323–10334.
- (38) Norman, P.; Bishop, D. M.; Jensen, H. J. A.; Oddershede, J. Nonlinear response theory with relaxation: The first-order hyperpolarizability. *The Journal of Chemical Physics* **2005**, *123*, 194103.
- (39) Ekström, U.; Norman, P.; Carravetta, V.; Ågren, H. Polarization Propagator for X-Ray Spectra. *Physical Review Letters* **2006**, *97*, 143001, Publisher: American Physical Society.
- (40) Coriani, S.; Fransson, T.; Christiansen, O.; Norman, P. Asymmetric-Lanczos-Chain-Driven Implementation of Electronic Resonance Convergent Coupled-Cluster Linear Response Theory. *Journal of Chemical Theory and Computation* **2012**, *8*, 1616–1628, Publisher: American Chemical Society.
- (41) Coriani, S.; Christiansen, O.; Fransson, T.; Norman, P. Coupled-cluster response theory for near-edge x-ray-absorption fine structure of atoms and molecules. *Physical Review A* **2012**, *85*, 022507, Publisher: American Physical Society.
- (42) Pedersen, M. N.; Hedegård, E. D.; Olsen, J. M. H.; Kauczor, J.; Norman, P.; Kongsted, J. Damped Response Theory in Combination with Polarizable Environments: The Polarizable Embedding Complex Polarization Propagator Method. *Journal of Chemical Theory and Computation* **2014**, *10*, 1164–1171, Publisher: American Chemical Society.
- (43) Riesz, F.; Sz.-Nagy, B. *Functional Analysis*; Courier Corporation, 2012; Google-Books-ID: JCfEAqAAQBAJ.
- (44) Polizzi, E. Density-matrix-based algorithm for solving eigenvalue problems. *Physical Review B* **2009**, *79*, 115112.



- (45) Di Napoli, E.; Polizzi, E.; Saad, Y. Efficient estimation of eigenvalue counts in an interval. *Numerical Linear Algebra with Applications* **2016**, *23*, 674–692, eprint: <https://onlinelibrary.wiley.com/doi/pdf/10.1002/nla.2048>.
- (46) Baiardi, A.; Kelemen, A. K.; Reiher, M. Excited-State DMRG Made Simple with FEAST. *Journal of Chemical Theory and Computation* **2022**, *18*, 415–430, Publisher: American Chemical Society.
- (47) Takahira, S.; Ohashi, A.; Sogabe, T.; Usuda, T. S. Quantum algorithm for matrix functions by Cauchy’s integral formula. *Quantum Information and Computation* **2020**, *20*, 14–36, arXiv:2106.08075 [quant-ph].
- (48) Hummel, F. Finite Temperature Coupled Cluster Theories for Extended Systems. *Journal of Chemical Theory and Computation* **2018**, *14*, 6505–6514, Publisher: American Chemical Society.
- (49) White, A. F.; Chan, G. K.-L. A Time-Dependent Formulation of Coupled-Cluster Theory for Many-Fermion Systems at Finite Temperature. *Journal of Chemical Theory and Computation* **2018**, *14*, 5690–5700, Publisher: American Chemical Society.
- (50) Harsha, G.; Henderson, T. M.; Scuseria, G. E. Thermofield Theory for Finite-Temperature Coupled Cluster. *Journal of Chemical Theory and Computation* **2019**, *15*, 6127–6136, Publisher: American Chemical Society.
- (51) Deutsch, J. M. Quantum statistical mechanics in a closed system. *Physical Review A* **1991**, *43*, 2046–2049, Publisher: American Physical Society.
- (52) Srednicki, M. Chaos and quantum thermalization. *Physical Review E* **1994**, *50*, 888–901, Publisher: American Physical Society.
- (53) Rigol, M.; Dunjko, V.; Olshanii, M. Thermalization and its mechanism for generic isolated quantum systems. *Nature* **2008**, *452*, 854–858.

- (54) Deutsch, J. M. Eigenstate thermalization hypothesis. *Reports on Progress in Physics* **2018**, *81*, 082001, Publisher: IOP Publishing.
- (55) Irmejs, R.; Bañuls, M. C.; Cirac, J. I. Efficient Quantum Algorithm for Filtering Product States. *Quantum* **2024**, *8*, 1389, arXiv:2312.13892 [quant-ph].
- (56) Emrich, K. An extension of the coupled cluster formalism to excited states (I). *Nuclear Physics A* **1981**, *351*, 379–396.
- (57) Emrich, K. An extension of the coupled cluster formalism to excited states: (II). Approximations and tests. *Nuclear Physics A* **1981**, *351*, 397–438.
- (58) Harris, C. R. et al. Array programming with NumPy. *Nature* **2020**, *585*, 357–362, Number: 7825 Publisher: Nature Publishing Group.
- (59) Park, Y. C.; Perera, A.; Bartlett, R. J. Equation of motion coupled-cluster for core excitation spectra: Two complementary approaches. *The Journal of Chemical Physics* **2019**, *151*, 164117.
- (60) CCCBDB List calculated geometries, accessed on Aug 30, 2024. <https://cccbdb.nist.gov/geom1x.asp>.
- (61) Hicken, J. E.; Zingg, D. W. A Simplified and Flexible Variant of GCROT for Solving Nonsymmetric Linear Systems. *SIAM Journal on Scientific Computing* **2010**, *32*, 1672–1694, Publisher: Society for Industrial and Applied Mathematics.
- (62) Baker, A. H.; Jessup, E. R.; Manteuffel, T. A Technique for Accelerating the Convergence of Restarted GMRES. *SIAM Journal on Matrix Analysis and Applications* **2005**, *26*, 962–984, Publisher: Society for Industrial and Applied Mathematics.
- (63) Virtanen, P. et al. SciPy 1.0: fundamental algorithms for scientific computing in Python. *Nature Methods* **2020**, *17*, 261–272, Publisher: Nature Publishing Group.

- (64) Liao, K.; Schraivogel, T.; Luo, H.; Kats, D.; Alavi, A. Towards efficient and accurate ab initio solutions to periodic systems via transcorrelation and coupled cluster theory. *Physical Review Research* **2021**, *3*, 033072, Publisher: American Physical Society.
- (65) Liao, K.; Zhai, H.; Christlmaier, E. M.; Schraivogel, T.; Ríos, P. L.; Kats, D.; Alavi, A. Density Matrix Renormalization Group for Transcorrelated Hamiltonians: Ground and Excited States in Molecules. *Journal of Chemical Theory and Computation* **2023**, *19*, 1734–1743, Publisher: American Chemical Society.
- (66) Liao, K. nickirk/pymes at main. <https://github.com/nickirk/pymes/tree/main>.
- (67) Sun, Q.; Berkelbach, T. C.; Blunt, N. S.; Booth, G. H.; Guo, S.; Li, Z.; Liu, J.; McClain, J. D.; Sayfutyarova, E. R.; Sharma, S.; Wouters, S.; Chan, G. K.-L. PySCF: the Python-based simulations of chemistry framework. *Wiley Interdisciplinary Reviews: Computational Molecular Science* **2018**, *8*, Publisher: John Wiley & Sons, Ltd.
- (68) Sun, Q. et al. Recent developments in the PySCF program package. *The Journal of Chemical Physics* **2020**, *153*, 024109.
- (69) Sun, Q. Libcint: An efficient general integral library for Gaussian basis functions. *Journal of Computational Chemistry* **2015**, *36*, 1664–1671, reprint: <https://onlinelibrary.wiley.com/doi/pdf/10.1002/jcc.23981>.
- (70) Schirmer, J.; Trofimov, A. B.; Randall, K. J.; Feldhaus, J.; Bradshaw, A. M.; Ma, Y.; Chen, C. T.; Sette, F. *K*-shell excitation of the water, ammonia, and methane molecules using high-resolution photoabsorption spectroscopy. *Physical Review A* **1993**, *47*, 1136–1147.
- (71) Brabec, J.; Bhaskaran-Nair, K.; Govind, N.; Pittner, J.; Kowalski, K. Communication: Application of state-specific multireference coupled cluster methods to core-level excitations. *The Journal of Chemical Physics* **2012**, *137*, 171101.

- (72) Sen, S.; Shee, A.; Mukherjee, D. A study of the ionisation and excitation energies of core electrons using a unitary group adapted state universal approach. *Molecular Physics* **2013**, *111*, 2625–2639, Publisher: Taylor & Francis eprint: <https://doi.org/10.1080/00268976.2013.802384>.
- (73) Dutta, A. K.; Gupta, J.; Vaval, N.; Pal, S. Intermediate Hamiltonian Fock Space Multireference Coupled Cluster Approach to Core Excitation Spectra. *Journal of Chemical Theory and Computation* **2014**, *10*, 3656–3668, Publisher: American Chemical Society.
- (74) Myhre, R. H.; Wolf, T. J. A.; Cheng, L.; Nandi, S.; Coriani, S.; Gühr, M.; Koch, H. A theoretical and experimental benchmark study of core-excited states in nitrogen. *The Journal of Chemical Physics* **2018**, *148*, 064106.
- (75) Domke, M.; Xue, C.; Puschmann, A.; Mandel, T.; Hudson, E.; Shirley, D. A.; Kaindl, G. Carbon and oxygen K-edge photoionization of the CO molecule. *Chemical Physics Letters* **1990**, *173*, 122–128.
- (76) Ma, Y.; Chen, C. T.; Meigs, G.; Randall, K.; Sette, F. High-resolution K-shell photoabsorption measurements of simple molecules. *Physical Review A* **1991**, *44*, 1848–1858, Publisher: American Physical Society.
- (77) Carbone, J. P.; Cheng, L.; Myhre, R. H.; Matthews, D.; Koch, H.; Coriani, S. *An analysis of the performance of coupled cluster methods for core excitations and core ionizations using standard basis sets*; 2019; Vol. 79; pp 241–261, arXiv:1908.03635 [physics].
- (78) Guthrie, K.; Dobrutz, W.; Gunnarsson, O.; Alavi, A. Time Propagation and Spectroscopy of Fermionic Systems Using a Stochastic Technique. *Physical Review Letters* **2018**, *121*.
- (79) Haegeman, J.; Cirac, J. I.; Osborne, T. J.; Pižorn, I.; Versnel, H.; Verstraete, F.

- Time-Dependent Variational Principle for Quantum Lattices. *Physical Review Letters* **2011**, *107*, 070601, Publisher: American Physical Society.
- (80) Haegeman, J.; Lubich, C.; Oseledets, I.; Vandereycken, B.; Verstraete, F. Unifying time evolution and optimization with matrix product states. *Physical Review B* **2016**, *94*, 165116, Publisher: American Physical Society.
- (81) Xu, Y.; Xie, Z.; Xie, X.; Schollwöck, U.; Ma, H. Stochastic Adaptive Single-Site Time-Dependent Variational Principle. *JACS Au* **2022**, *2*, 335–340, Publisher: American Chemical Society.
- (82) Yang, M.; White, S. R. Time-dependent variational principle with ancillary Krylov subspace. *Physical Review B* **2020**, *102*, 094315, Publisher: American Physical Society.
- (83) Ronca, E.; Li, Z.; Jimenez-Hoyos, C. A.; Chan, G. K.-L. Time-step targeting time-dependent and dynamical density matrix renormalization group algorithms with ab initio Hamiltonians. *Journal of Chemical Theory and Computation* **2017**, *13*, 5560–5571, arXiv:1706.09537 [cond-mat, physics:physics].
- (84) Grundner, M.; Westhoff, P.; Kugler, F. B.; Parcollet, O.; Schollwöck, U. Complex time evolution in tensor networks and time-dependent Green’s functions. *Physical Review B* **2024**, *109*, 155124, Publisher: American Physical Society.